SIMULATING COMPRESSIBLE AND INCOMPRESSIBLE FLOWS USING A NEW HIGH RESOLUTION UPWIND CONVECTION SCHEME

Laís Corrêa, lacorrea@icmc.usp.br
Giseli Ap. Braz de Lima, giabl@icmc.usp.br
Valdemir Garcia Ferreira, pvgf@icmc.usp.br
Instituto de Ciências Matemáticas e de Computação - USP, Av. Trabalhador São-carlense, 400 - CEP: 13560-970 - São Carlos - SP.

Abstract. *Convection schemes of high resolution are extensively used nowadays to solve fluid dynamics problems, especially the incompressible class of flows involving high values of Reynolds number with moving free surfaces. Numerical solutions for this class of problems are difficult to find, because of the strong influence of nonlinear convective terms in the transport equations. Consequently, the choice of the numerical method that takes into account the flow direction (upwinding) has atracted many researchers in the modern CFD community. In this sense and with these motivations, we present in this work a new high resolution polynomial upwind convection scheme, called EPUS (Eight-degree Polynomial Upwind Scheme), for the numerical solution of systems of conservation laws and related fluid dynamics problems. The new scheme is developed by using a polynomial of eight-degree in the context of normalized variables of Leonard, that satisfies the CBC (Convection Boundedness Criterion) and TVD (Total Variation Diminishing) stability criteria. An important property of the high resolution EPUS scheme is to be as accurate as possible in smooth regions and with controled numerical dissipation in regions of high gradients and discontinuities. The performance of the EPUS scheme is assessed in the numerical solution of compressible Euler and shallow water equations. As application, the scheme is then used for solving incompressible Navier-Stokes equations; in particular, the numerical solutions of the circular hydraulic jump and broken-dam problems are presented. The numerical results confirm that the EPUS scheme is an effective tool for resolving both compressible and incompressible complex flow problems.*

Keywords: *upwinding, convection terms, Navier-Stokes equations, conservation laws*

1. INTRODUCTION

High resolution upwind convection schemes are extensively used today to solve problems in fluid dynamics, especially for the class of non-stationary incompressible flow problems involving moving free surfaces at high values of Reynolds number. It has been difficult to obtain representative numerical solutions for these problems due to the strong influence of the convective terms (in general nonlinear) in the transport equations. Because of this, several attemps have been made in this direction by researchers in CFD community. The major obstacle has been developing a scheme that captures discontinuities, achieves high accuracy (in general ≥ 2), is stable, preserves monotonicity, is economic and is easy to implement.

We presented in this work a new high resolution polynomial convection scheme using the upwind strategy for the discretization of the linear and nonlinear convection terms. The new scheme, called EPUS (Eight-degree Polynomial Upwind Scheme), is based on the Normalized Variable (NV) formulation of Leonard (1988) and satisfies the Total Variation Diminishing (TVD) of Harten (1983) and Convection Boundedness Criterion (CBC) of Gaskell and Lau (1988) for stability.

A brief description of the scheme is done and then numerical results are presented for 1D and 2D hyperbolic conservation laws. As application, the EPUS scheme is used for the simulation of non-stationary incompressible flow problems involving moving free surfaces, which are modeled by Navier-Stokes equations. The numerical results show that the new upwinding scheme performs very well.

2. THEORETICAL BASE FOR THE DEVELOPMENT OF A HIGH RESOLUTION UPWIND SCHEME

In the upwind strategy, the convective terms are approximated according to the convection velocity. For this, it is considered three computational nodes adjacent to the point of discretization, ie, the downstream D, the upstream U and the remote-upstream R. Figure 1 illustrates this strategy, where one can observe that the positions of D, U and R are adopted in accordance with the sign of the convection velocity V_f in the face f of a convected variable ϕ_f. A scheme that adopts this strategy is written in the following form (in general nonlinear):

$$\phi_f = \phi_f(D, U, R). \tag{1}$$

In order to simplify the functional relationship given by Eq. (1), linking ϕ_D, ϕ_U and ϕ_R, the original variables are transformed in NV of Leonard (1988) as

$$\hat{\phi_{()}} = \frac{\phi_{()} - \phi_R}{\phi_D - \phi_R}. \tag{2}$$

Figure 1. Position of computational nodes D, U and R according to the sign of velocity V_f of a convected variable ϕ_f.

From this definition it is observed that $\hat{\phi}_R = 0$ and $\hat{\phi}_D = 1$. Thus, we conclude that any convection upwind scheme using only the values of ϕ at points D, U and R can be represented in the functional form

$$\hat{\phi}_f = \hat{\phi}_f(\hat{\phi}_U). \tag{3}$$

In this context, Leonard (1988) showed that any nonlinear (or piecewise linear) monotonic scheme formulated in NV, with $0 \leq \hat{\phi}_U \leq 1$, must satisfy the following conditions: pass through the points $O(0,0)$ and $P(1,1)$ (to be monotonic), pass through the point $Q(0.5, 0.75)$ (to reach second order of accuracy) and pass through the point Q with inclination of 0.75 (to reach third order of accuracy). Leonard also recommends that for values of $\hat{\phi}_U < 0$ or $\hat{\phi}_U > 1$, the scheme must be extended in a continuous manner using the FOU (First Order Upwinding) scheme, which is defined by $\hat{\phi}_f = \hat{\phi}_U$.

Bounded solution (stability) is reached by considering the CBC of Gaskell and Lau (1988), namely:

$$-\ \hat{\phi}_U \leq \hat{\phi}_f(\hat{\phi}_U) \leq 1, \qquad \text{if } \hat{\phi}_U \in [0,1]; \tag{4}$$

$$-\hat{\phi}_f = \hat{\phi}_f(\hat{\phi}_U) = \hat{\phi}_U, \qquad \text{if } \hat{\phi}_U \notin [0,1]; \tag{5}$$

$$-\hat{\phi}_f(0) = 0 \text{ and } \hat{\phi}_f(1) = 1. \tag{6}$$

Another important stability criterion is the TVD constraint of Harten (1983). This property ensures that, in general, spurious oscillations (unphysical noises) are removed from the numerical solution. Formally, consider a sequence of discrete approximations $\phi(t) = \phi_i(t)_{i\in\mathbf{Z}}$ for a scalar quantity. The Total Variation (TV) at time t of this sequence is defined by

$$TV(\phi(t)) = \sum_{i\in\mathbf{Z}} |\phi_{i+1}(t) - \phi_i(t)|. \tag{7}$$

From this, by definition, we say that a scheme is TVD if, for all data set ϕ^n, the values ϕ^{n+1} calculated by numerical method satisfy

$$TV(\phi^{n+1}) \leq TV(\phi^n), \quad \forall n. \tag{8}$$

It is important to emphasize, from numerical point of view, that TVD schemes are very attractive, since they guarantee monotonicity and convergence .

3. THE EPUS SCHEME

The EPUS scheme is developed by assuming that the NV $\hat{\phi}_f$ at the cell interface f is related to $\hat{\phi}_U$ as part of an eight-degree polynomial function

$$\hat{\phi}_f = \sum_{k=0}^{8} a_k \hat{\phi}_U^k, \tag{9}$$

for $0 \leq \hat{\phi}_U \leq 1$, and the FOU scheme for $\hat{\phi}_U < 0$ or $\hat{\phi}_U > 1$. By considering the coefficient a_3 as a free parameter, say λ, the other coefficients in Eq. (9) are determined by imposing the four conditions of Leonard (1988) presented above, plus the condition that this polynomial function must be of C^2 class (ie, it possesses first and second derivate continuously differentiable). For this, the polynomial function is linked at the points $(0,0)$ and $(1,1)$ with the same values of the first and second derivatives of the FOU scheme. This differentiability condition is imposed because schemes of C^1 class avoid convergence problems when coarse meshes are employed (see Lin and Chieng (1991)). In this sense, we propose a new polynomial upwinding scheme (the EPUS scheme) as being an original function of C^2 class in an attempt to obtain good results (the numerical results confirmed our supposition).

In summary, the EPUS scheme with the free parameter λ in its formulation, in NV, is given by

$$\hat{\phi}_f = \begin{cases} -4(\lambda\text{–}24)\hat{\phi}_U^8 + 16(\lambda\text{–}23)\hat{\phi}_U^7 + (528\text{–}25\lambda)\hat{\phi}_U^6 + (19\lambda\text{–}336)\hat{\phi}_U^5 + (80\text{–}7\lambda)\hat{\phi}_U^4 + \lambda\hat{\phi}_U^3 + \hat{\phi}_U, & \text{if} \quad \hat{\phi}_U \in [0,1], \\ \hat{\phi}_U, & \text{if} \quad \hat{\phi}_U \notin [0,1]. \end{cases} \tag{10}$$

The corresponding flux limiter function for the EPUS scheme is derived rewritten Eq. (10) (see Waterson and Deconinck (2007)) as

$$\hat{\phi}_f = \hat{\phi}_U + \frac{1}{2}\psi_f(1 - \hat{\phi}_U), \tag{11}$$

where $\psi_f = \psi(r_f)$ is the flux limiter function and r_f is the ratio of consecutive gradients (a sensor). In NV, this sensor is given by

$$r_f = \frac{\hat{\phi}_U}{1 - \hat{\phi}_U}. \tag{12}$$

By combining Eqs. (10), (11) and (12), we deduce the flux limiter function for the EPUS scheme. The result is

$$\psi(r_f) = \begin{cases} \frac{(2\lambda-32)r_f^5 + (160-4\lambda)r_f^4 + 2\lambda r_f^3}{(1+r_f)^7}, & \text{if} \quad r_f \geq 0, \\ 0, & \text{if} \quad r_f < 0, \end{cases} \tag{13}$$

or, for the computational implementation, as

$$\psi(r_f) = \max\left\{0, \frac{0.5(|r_f| + r_f)[(2\lambda-32)r_f^4 + (160-4\lambda)r_f^3 + 2\lambda r_f^2]}{(1+|r_f|)^7}\right\}. \tag{14}$$

It is important to observe that the EPUS scheme is TVD for the free parameter $\lambda \in [16, 95]$, and for λ in this interval we can define the free parameter according to the problem at hand. In this work, two particular values were selected, namely $\lambda = 16$ and 95. From several numerical tests, it was observed that the lower bound of the range of parameters, ie $\lambda = 16$, is the parameter has lead to better performance of the EPUS scheme in problems with smooth initial conditions. While for the upper bound $\lambda = 95$, best results are achieved by the scheme EPUS in problems with discontinuities, extreme points and high gradients. Figure 2 shows the EPUS scheme in TVD region for the free parameters $\lambda = 16$ e 95, being Fig. 2 (a) in the $\hat{\phi}_U \perp \hat{\phi}_f$ plan and Fig. 2 (b) in the $r_f \perp \psi_f$ plan.

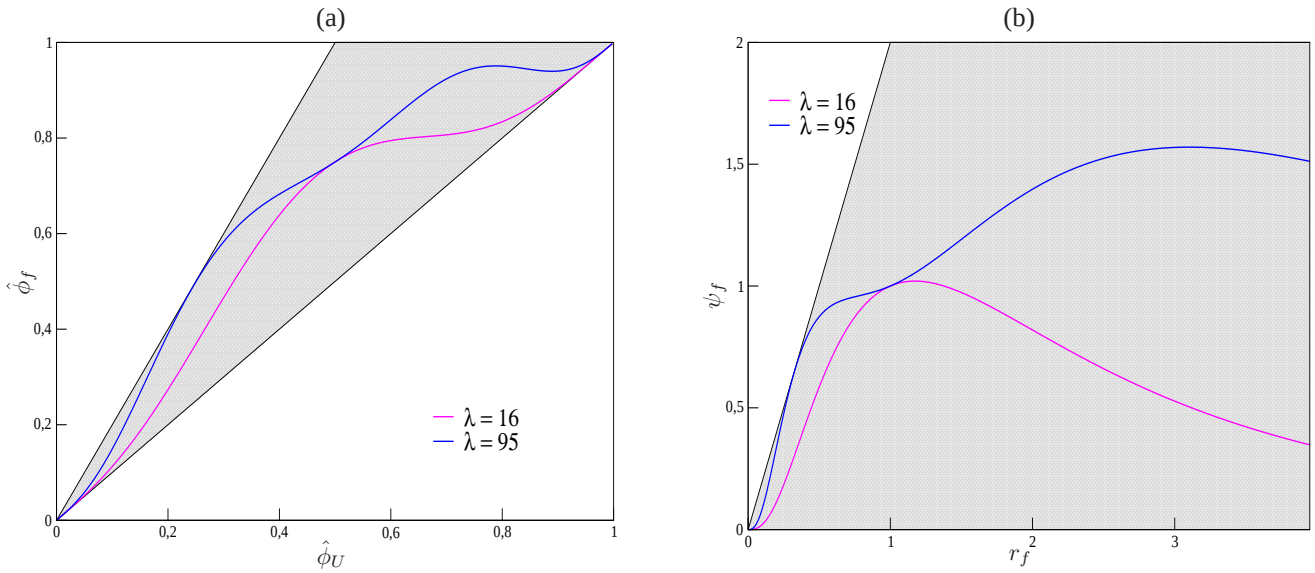

Figure 2. EPUS scheme (a) in normalized variables and (b) in the flux limiter form in TVD region.

Note that the EPUS scheme is monotonic and reaches second order of accuracy, since its flux limiter function, for $r_f \geq 0$, satisfies the condition introduced by Waterson and Deconinck (2007), namely a scheme must respect the linear variation of the solution, satisfying $\psi(1) = 1$, which is also a necessary condition for achieving second order accuracy on uniform meshes. In addition, the EPUS scheme can reach third order accuracy, since its flux limiter function, for $r_f \geq 0$, satisfies $\psi'(1) = \frac{1}{4}$ (see Zijlema (1996)), which is a necessary and sufficient condition for obtaining third order accuracy.

4. NUMERICAL RESULTS

In order to evaluate the EPUS scheme (verify its behavior, flexibility and robustness), from now on we solve various nonlinear conservation laws, such as 1D Euler, 2D shallow water and axisymmetric/3D Navier-Stokes equations. For Euler and shallow water equations, we have used the well recognized CLAWPACK[1] (Conservation LAW PACKage) software of LeVeque. This package uses the Godunov method with a correction term equipped with a flux limiter (see LeVeque (2002)). For solving axisymmetric/3D Navier-Stokes equations, we have employed the genuinely Brazilian Freeflow code of Castelo *et al.* (2000) equipped with EPUS scheme.

4.1 1D Euler equations

These equations are given by

$$\phi_t + F(\phi)_x = 0, \tag{15}$$

where $\phi = [\rho, \rho u, E]^T$ represents the conserved variable vector and $F(\phi) = [\rho u, \rho u^2 + p, (E+p)u]^T$ is the flux function vector, being ρ the density, p the pressure, ρu the momentum and E the total energy. To close the system, it was considered the ideal gas equation

$$p = (\gamma - 1)(E - \frac{1}{2}\rho u^2), \tag{16}$$

where $\gamma = 1.4$ is the ratio of specific heat. The problem to be simulated here is a challenger Riemann problem proposed by Woodward and Collela (1984), known as "Two Interacting Blast Waves", which involves multiple interactions of strong shocks. The initial condition is given by

$$(\rho_0,\ u_0,\ p_0)^T = \begin{cases} (1,\ 0,\ 1000)^T, & \text{if} \quad 0 \leq x \leq 0.1, \\ (1,\ 0,\ 0.01)^T, & \text{if} \quad 0.1 < x \leq 0.9, \\ (1,\ 0,\ 100)^T, & \text{if} \quad 0.9 < x \leq 1.0. \end{cases} \tag{17}$$

The numerical solution was obtained by CLAWPACK software equipped with the flux limiter EPUS in a mesh size of 1000 computational cells, at $\theta = 0.9$ and final time $t = 0.038$. The reference solution, as suggested by LeVeque in the CLAWPACK, was generated by the MC limiter in a mesh size of 2000 computational cells, at $\theta = 0.9$ and final time $t = 0.038$. Figures 3 and 4 show a comparison between the reference and numerical solutions, where it can seen that the EPUS scheme provides solutions in good agreement with the reference one, although introducing small numerical viscosity in some regions.

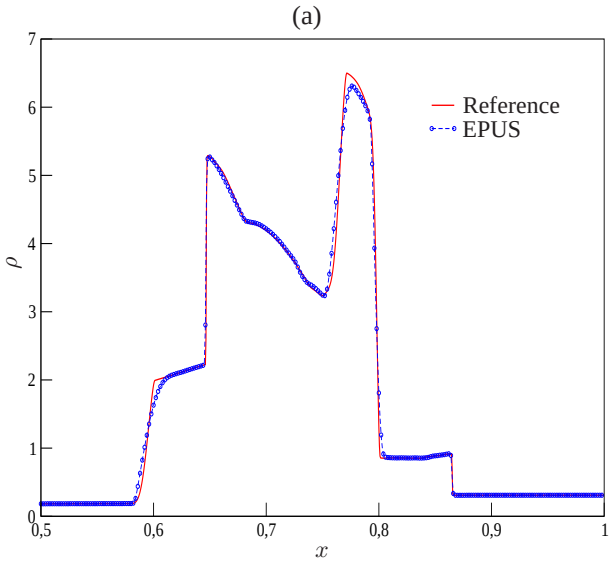

Figure 3. Reference and numerical solutions for 1D Euler equations using the "Two Interacting Blast Waves" for (a) density, (b) total energy and (c) velocity.

In order to evaluate a EPUS scheme in the quantitative sense, we calculate the relative error and the convergence order for this problem using the norm-1. The results obtained are presented in Tab. 1, in which it is possible to observe that the new scheme reaches the formal convergence order (up to order 3).

[1] http://www.amath.washington.edu/∼claw/

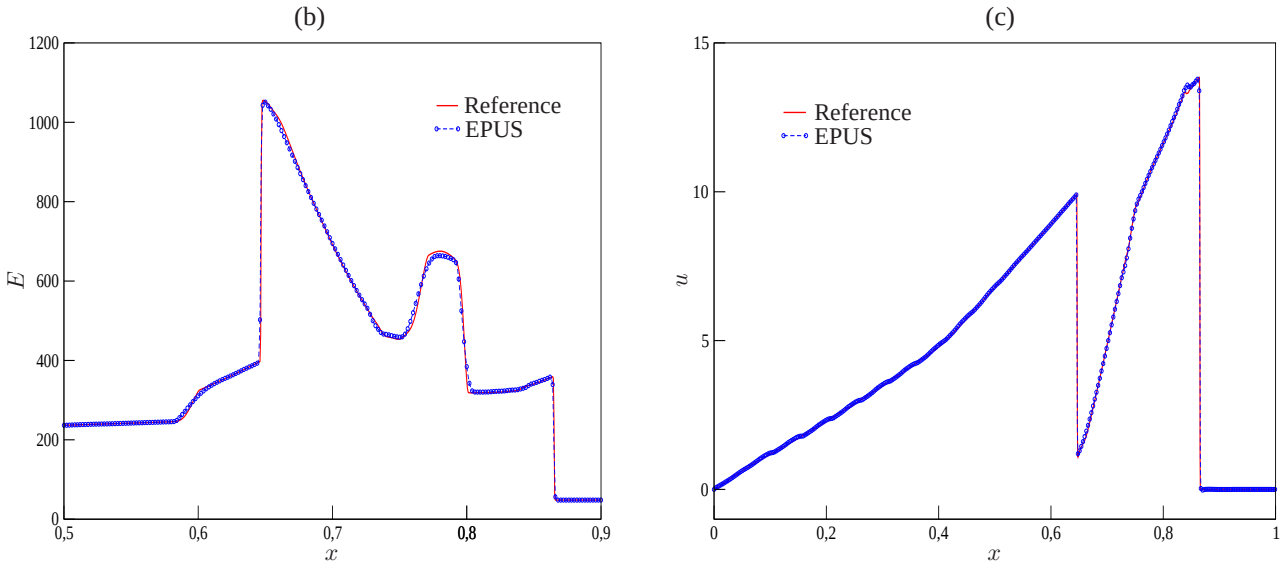

Figure 4. Continuation of Fig. 3.

Table 1. Relative error and convergence order for the EPUS scheme using the "Two Interacting Blast Waves" problem.

Mesh Size	Relative Error (norm-1)	Convergence Order
125	0.186900	—
250	0.098291	0.927138
500	0.041372	1.248393
1000	0.012660	1.708353

4.2 2D Shallow water equations

The 2D nonlinear hyperbolic shallow water equations are given by

$$\phi_t + F(\phi)_x + G(\phi)_y = 0, \tag{18}$$

with $\phi = [h, hu, hv]^T$ the conserved variable vector, and $F(\phi) = [hu, hu^2 + \frac{1}{2}gh^2, huv]^T$ and $G(\phi) = [hu, huv, hv^2 + \frac{1}{2}gh^2]^T$ the flux function vectors in the directions x e y, respectively. $h = h(x, y, t)$ represents the height of the fluid, $[u, v]^T$ and $[hu, hv]^T$ are, respectively, the velocity and discharge vectors, and g is the acceleration due to gravity. The performance of the EPUS scheme for solving this hyperbolic system is verified by simulating the radial dam-break problem (see LeVeque (2002)). In summary, this problem consists in a circular fluid portion initially at rest confined by a dam (see Fig. 5 (a)), in the domain $[-2.5, 2.5] \times [-2.5, 2.5]$. The dam is instantly removed forming a shock wave, that travels radially outwards while a rarefaction wave propagates inwards (see Fig. 5 (b)). Initially, the height of fluid inside of dam is $h = 2$ and outside is $h = 1$. According to LeVeque (2002), this problem is similar to the structure of the 1D Riemann problem for the dam-break. Taking into account this statement, we consider the solution of this 1D problem as a reference solution for the 2D case. The solution is calculated by solving the following 1D shallow water system with source term:

$$\begin{aligned} h_t + (hU)_r &= -\frac{hU}{r}, \\ (hU)_t + \left(hU^2 + \frac{1}{2}gh^2\right)_r &= -\frac{hU^2}{r}, \end{aligned} \tag{19}$$

where $U(r, t)$ is the radial velocity and h is the height as a function of r (distance from the origin).

For the simulation of this problem, we consider, for the numerical solution, Courant number $\theta = 0.9$ and a mesh size of 125×125 computational cells, while the reference solution was calculated using a mesh size of 2000 computational cells. The results for the h contours, in the $x \perp y$ plan and final time $t = 1.5$, are shown in Fig. 6 (a). In order to complete the analysis, we calculated the height variation as a function of distance from the origin (ie, h in line $y = 0$), as shown in Fig. 6 (b), which compares the EPUS scheme with the reference solution, showing that the new scheme has good performance.

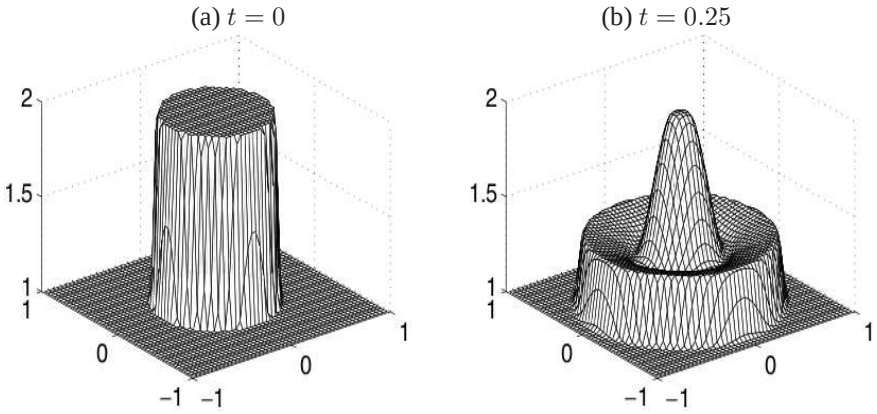

Figure 5. Radial dam-break problem: behavior of the height of the fluid portion in times (a) $t = 0$ e (b) $t = 0.25$ (figure extracted from LeVeque (2002)).

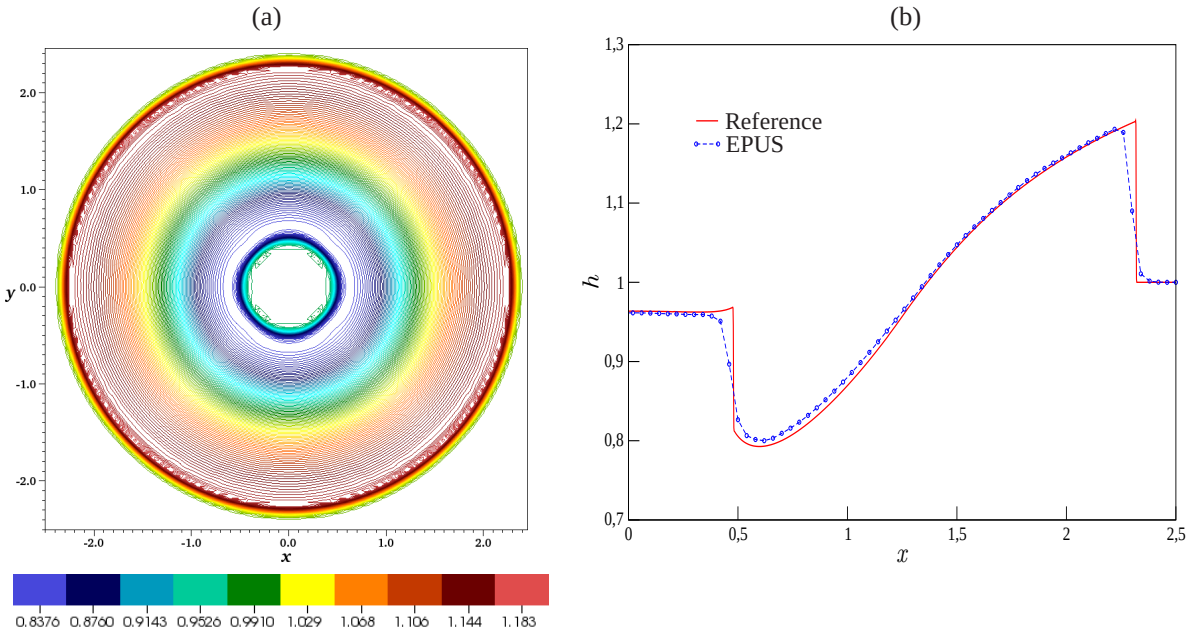

Figure 6. h profiles for the radial dam-break problem: (a) reference and (b) numerical (EPUS) solutions.

4.3 Axisymmetric Navier-Stokes equations

In this section, as an application, we evaluate the EPUS scheme by solving laminar incompressible fluid flows involving a moving free surface, which are modeled by the axisymmetric Navier-Stokes equations. For this, we considered a vertical free jet impinging perpendiculary onto an impermeable rigid surface (under the action of gravitational field), leading to the formation of a curious phenomenon known as circular hydraulic jump (see, for example, Rai *et al.* (2008)). These instantaneous equations are given by

$$\frac{\partial u}{\partial t} + \frac{1}{r}\frac{\partial (ruu)}{\partial r} + \frac{\partial (uv)}{\partial z} = -\frac{\partial p}{\partial r} + \frac{1}{Re}\frac{\partial}{\partial z}\left(\frac{\partial u}{\partial z} - \frac{\partial v}{\partial r}\right) + \frac{g_r}{Fr^2}, \tag{20}$$

$$\frac{\partial v}{\partial t} + \frac{1}{r}\frac{\partial (rvu)}{\partial r} + \frac{\partial (vv)}{\partial z} = \frac{\partial p}{\partial z} + \frac{1}{Re}\frac{1}{r}\frac{\partial}{\partial r}\left(r\left(\frac{\partial u}{\partial z} - \frac{\partial v}{\partial r}\right)\right) + \frac{g_z}{Fr^2}, \tag{21}$$

$$\frac{1}{r}\frac{\partial (ru)}{\partial r} + \frac{\partial v}{\partial z} = 0, \tag{22}$$

where t is time, $u = u(r, z, t)$ and $v = v(r, z, t)$ are, respectively, the components of velocity vector in the r and z directions and $g = (g_r, g_z)^T$ is the acceleration due to gravity. The dimensionless parameters $Re = U_0 L_0/\nu$ and $Fr = U_0/\sqrt{L_0 g}$ represent, respectively, the Reynolds and Froud numbers, with ν being the coefficient of kinematic viscosity given by $\nu = \mu/\rho$, where μ is the dynamic viscosity. Finally, U_0 and L_0 are characteristic scales for velocity

and length, respectively.

A viscous analytical solution for this problem was calculated by Watson (1964), for the total thickness of the fluid layer H. For this, Watson divided the fluid flow in four regions (see Watson (1964)): (i) when $r = O(a)$, the speed outside the boundary layer rises rapidly from 0 at the stagnation point to U_0 and the boundary layer thickness is $\delta = O(\nu a/U_0)^{1/2}$, with a being the impinging jet radius; (ii) for $r \gg a$, where the conditions in region (i) do not affect the flow and the boundary layer remains almost constant (equal to U_0), also the velocity distribution has the Blasius profile and the boundary layer thickness is $O(\nu a/U_0)^{1/2}$; (iii) from the point where the boundary layer absorbs the layer of fluid to the point where the velocity profile becomes self-similar; (iv) at large distances from the stagnation point where the final similarity solution is valid. According to Watson (1964), the viscous analytical solution is valid only in (ii) and (iv) regions for the Reynolds number $Re = Q/\nu a \gg 1$, with $Q = \pi a^2 U_0$ being the discharge of flow. It is worth adding that his approximate solution is not applicable in the neighborhoods of the stagnation point. The viscous analytical solution of Watson is given by:

$$H(r) = \begin{cases} \frac{a^2}{2r} + \left(1 - \frac{2\pi}{3\sqrt{3}c^2}\right)\delta, & r < r_0, \\ \frac{2\pi^2}{3\sqrt{3}}\frac{\nu(r^3+l^2)}{Qr}, & r \geq r_0, \end{cases} \tag{23}$$

in which

$$\delta^2 = \frac{\pi\sqrt{3}c^3}{\pi - c\sqrt{3}}\frac{\nu r a^2}{Q}, \tag{24}$$

where $c = 1.402$, $r_0 = 0.3155 a Re^{\frac{1}{3}}$ and l is an arbitrary constant which was estimated by considering the initial development of the boundary layer to be $l = 0.567 a Re^{\frac{1}{3}}$.

For the simulation, we considered the following data:

– Mesh I: 800×504 computational cells;
– Mesh II: 400×252 computational cells;
– Mesh III: 200×126 computational cells;
– Domain: $0.050m \times 0.0315m$;
– Jet radius $r_i = 0.004m$;
– Jet height $h_i = 0.00075m$;
– Length scale: $L_0 = 2r_i = 0.008m$;
– Velocity scale: $U_0 = 0.375m/s$;
– Coefficient of kinematic viscosity: $\nu = 1.2 \cdot 10^{-5} m^2/s$;
– Reynolds number: $Re = 250$.

Figure 7 shows the comparison between the viscous analytical solution of Watson and the numerical solutions obtained with the EPUS scheme, in the meshes Mesh I, Mesh II and Mesh III. This figure also depicts, for simple illustration, the boundary layer thickness δ by Watson. From the figure, one can conclude that the solution obtained with the EPUS scheme is in agreement with the analytical solution (in the region where it is valid). As illustration, Fig. 8 (a) presents an experiment of the circular hydraulic jump, which is used for comparison with the 3D result obtained with the EPUS scheme. From these figures, one can observe that the new scheme shows good performance for solving this problem.

A quantitative analysis is also done in this test. For this, we compare the radius of the circular hydraulic jump calculated with the EPUS scheme and the theoretical approach of Brechet and Néda (1999)

$$R = \left(\frac{27 g^{-1/4}}{2^{1/4} 35\pi}\right)^{\frac{2}{3}} Q^{2/3} d^{-1/6} \nu^{-1/3}, \tag{25}$$

in which d represents the height between the rigid surface and the jet. The results for the jump radius are presented in Tab. 2, from which we conclude that when the mesh is refined, the calculated jump radius using the EPUS scheme converges to the theoretical approach.

Table 2. Comparison of the results for the jump radius obtained with the EPUS scheme and with the theoretical approach of Brechet and Néda (1999).

Mesh Size	Theoretical Approximation	Results by EPUS
Mesh I	1.325158 e-2	1.783112 e-2
Mesh II	1.325158 e-2	1.638573 e-2
Mesh III	1.325158 e-2	1.414912 e-2

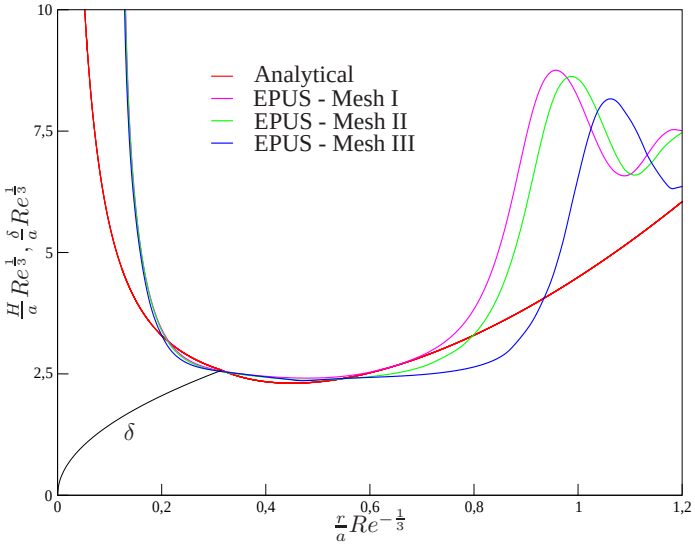

Figure 7. Comparison of the solutions for the circular hydraulic jump problem.

(a) (b)

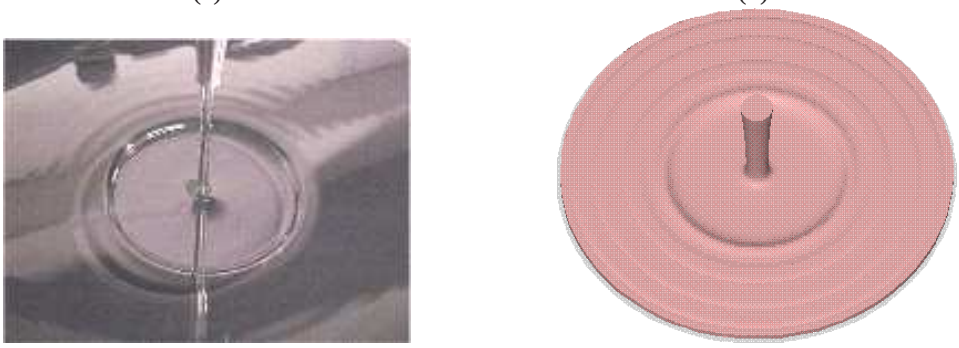

Figure 8. Illustration of circular hydraulic jump: (a) experimental and (b) numerical (EPUS) results.

We concluded this test by showing the convergence order with the EPUS scheme. For this we used the meshes Mesh I, Mesh II e Mesh III and the mathematical relationship of Jameson and Martinelli (1998). The calculated value is

$$\log_2 \left| \frac{R_{MeshI} - R_{MeshII}}{R_{MeshII} - R_{MeshIII}} \right| = 1.90. \tag{26}$$

Note that the convergence order obtained with the EPUS scheme, for this complex free surface flow, is consistent with the formal order of accuracy of the scheme.

4.4 3D Navier-Stokes equations

The instantaneous 3D Navier-Stokes equations, in Einstein notation, are given by

$$\frac{\partial u_i}{\partial t} + \frac{\partial (u_i u_j)}{\partial x_j} = -\frac{\partial p}{\partial x_i} + \frac{1}{Re}\frac{\partial}{\partial x_j}\left(\frac{\partial u_i}{\partial x_j}\right) + \frac{1}{Fr^2} g_i, \quad i = 1, 2, 3 \tag{27}$$

$$\frac{\partial u_i}{\partial x_i} = 0, \tag{28}$$

where t is the time, $u = u(x, y, z)$ and $v = v(x, y, z)$ are, respectively, the components of velocity vector in the x, y and z directions and $g = (g_x, g_y, g_z)^T$ is the acceleration due to gravity.

We used these equations to model the broken-dam problem, which is caracterized by a moving free surface. This problem consists in a fluid block in hydrostatic equilibrium confined between impermeable rigid walls and under action of gravity. In $t = 0$ the fluid starts its moviment. The broken-dam problem was originally studied by Martin and Moyce (1952), which provided experimental data for the position of the fluid front x_{max}. Recently, numerical, theoretical and experimental data were also presented by Colagrossi and Landrini (2003).

For simulation of this problem, we used free-slip boundary condition and the following data:

– Mesh: $150 \times 50 \times 80$ computational cells;
– Domain: $0.3m \times 0.1m \times 0.16m$;
– Fluid block dimensions: $0.05m \times 0.1m \times 0.05m$;
– Length scale: $L_0 = 0.1m$;
– Velocity scale: $U_0 = \sqrt{gL_0} = 0.99045444m/s$;
– Coefficient of kinematic viscosity: $\nu = 10^{-6}m^2/s$;
– Reynolds number: $Re = 99045.444$.

Figure 9 shows the numerical solution obtained with the EPUS scheme for the position of the fluid front (x_{max}), which is compared with the data of Colagrossi and Landrini (2003). From this figure, one can observe that the new scheme presented satisfatory results, showing concordance with the literature data. In particular, the numerical solution obtained with the EPUS is the closest to the experimental results of Martin e Moyce.

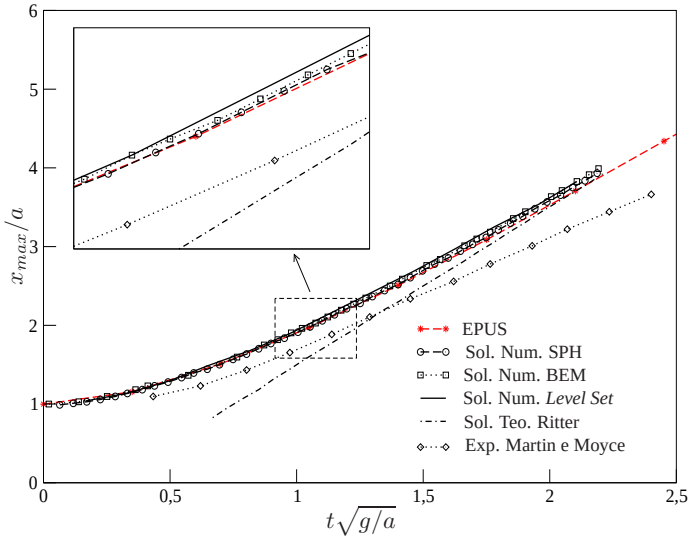

Figure 9. Comparison of the solutions for the 3D broken-dam problem.

For illustration, in Fig. 10 is presented the pressure field, showing the evolution of the moving free surface for the 3D broken-dam problem.

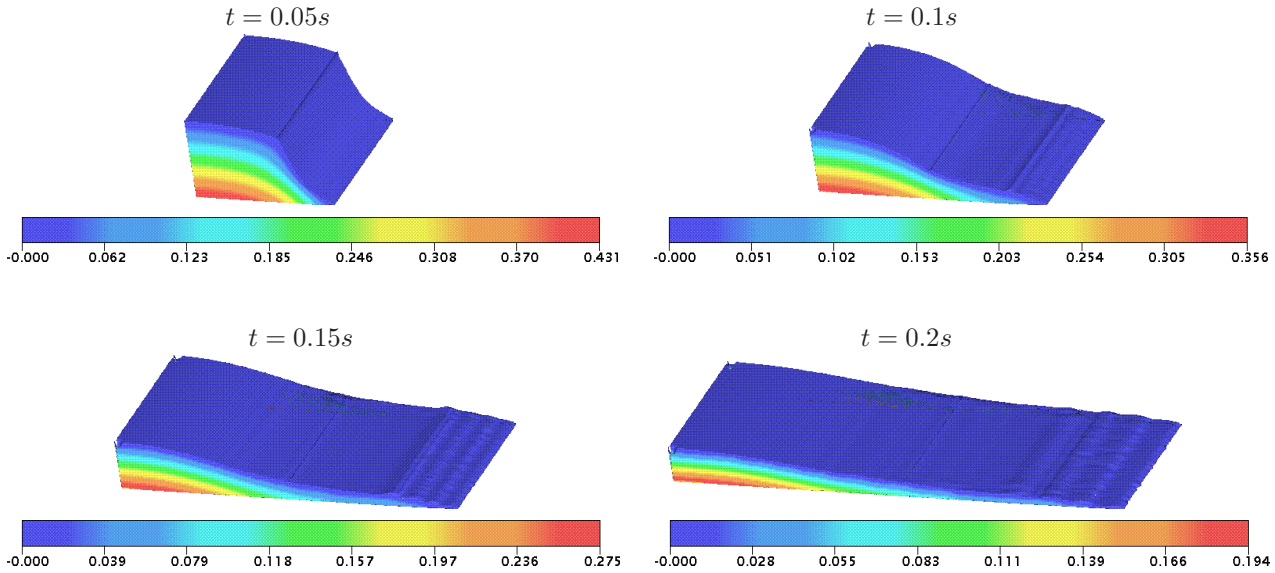

Figure 10. Pressure field for the broken-dam problem in different times.

5. CONCLUSION

In this article, we presented the EPUS scheme, a new high resolution upwind convection scheme for approximate nonlinear convection terms in non-stacionary fluid flows. The performance of the scheme was verified by solving various nonlinear problems, namely Euler, shallow water and Navier-Stokes equations. In all tests simulated, the results with the EPUS scheme presented good agreement with the numerical, reference, theoretical and experimental data, proving that this new upwind scheme can be considered a good tool for solving both compressible and incompressible fluid flows.

6. ACKNOWLEDGEMENTS

We gratefully acknowledge the support provided by FAPESP (Grants 2008/07367-9 and 2009/16954-8), CNPq (Grants 133446/2009-3, 300479/2008-5 and 573710/2008-2 (INCT-MACC)) and FAPERJ (Grant E-26/170.030/2008 (INCT-MACC)).

7. REFERENCES

Brechet, Y. and Néda, Z., 1999. "On the circular hydraulic jump". *American Journal of Physics*, Vol. 67.

Castelo, A.F., Tomé, M.F., César, C.N.L., McKee, S. and Cuminato, J.A., 2000. "Freeflow: An integrated simulation system for three-dimensional free-surface flows". *Journal of Computers and Visualization in Science*, Vol. 2, pp. 199–210.

Colagrossi, A. and Landrini, M., 2003. "Numerical simulation of interfacial flows by smoothed particle hydrodynamics". *Journal Computation Physics*, Vol. 191, pp. 448–475.

Gaskell, P.H. and Lau, A.K.C., 1988. "Curvature-compensated convective transport: SMART, a new boundedness preserving transport algorithm". *International Journal for Numerical Methods in Fluids*, Vol. 8, pp. 617–641.

Harten, A., 1983. "High resolution schemes for hyperbolic conservation laws". *Journal of Computational Physics*, Vol. 49, pp. 357–393.

Jameson, A. and Martinelli, L., 1998. "Mesh refinement and modeling errors in flow simulation". *AIAA Journal*, Vol. 36.

Leonard, B.P., 1988. "Simple high-accuracy resolution program for convective modelling of discontinuities". *International Journal for Numerical Methods in Fluids*, Vol. 8, pp. 1291–1318.

LeVeque, R.J., 2002. *Finite volume methods for hyperbolic problems*. University of Washington.

Lin, H. and Chieng, C., 1991. "Characteristic-based flux limiters of an essentially third-order flux-splitting method for hyperbolic conservation laws". *International Journal for Numerical Methods in Fluids*, Vol. 13, pp. 287–307.

Martin, J.C. and Moyce, W.J., 1952. "An experimental study of the collapse of liquid columns on a rigid horizontal plane". *Philosophical Transactions of the Royal Society, Mathematical, Phisical & Engeneering Sciences*, Vol. 244, pp. 312–324.

Rai, A., Dandapat, B.S. and Poria, S., 2008. "hydraulic jump in generalized-Newtonian fluids". *arXiv:0809.2231v3 [physics.flu-dyn]*.

Waterson, N.P. and Deconinck, H., 2007. "Design principles for bounded higher-order convection schemes - a unified approach". *Journal of Computational Physics*, Vol. 224, pp. 182–207.

Watson, E.J., 1964. "The radial spread of a liquid jet over a horizontal plane". *Journal of Fluid Mechanics*, Vol. 20, pp. 481–499.

Woodward, P. and Collela, P., 1984. "The numerical simulation of two-dimensional fluid flow with strong shocks". *Journal of Computational Phisics*, Vol. 54, pp. 115–173.

Zijlema, M., 1996. "On the construction of a third-order accurate monotone convection scheme with application to turbulent flows in general domains". *International Journal for Numerical Methods in Fluids*, Vol. 22, pp. 619–641.

8. Responsibility notice

The authors are the only responsible for the printed material included in this paper.